Active Noise Control Headphones

André Cerqueira, Paulo Lopes
andre.cerqueira@ist.utl.pt
Instituto Superior Técnico, ULisboa, Lisboa, Portugal

November 2016

Abstract

In acoustic active noise control (ANC), an unwanted noise is acquired by a microphone, processed and an "anti-noise", with the opposite phase from the original noise, is emitted by a loudspeaker. The anti-noise is superimposed to the original signal and destructive interference occurs. This paper presents the design, implementation and results of an adaptive ANC headphone system. A TMS320C6713 floating-point digital signal processor was used as the controller. Various algorithms were employed and performance has been evaluated and compared between them and with reported results in the literature.
Keywords: Active Noise Control (ANC), ANC Headset, Adaptive ANC systems, Digital signal processing, LMS Algorithm

1. Introduction

Earmuffs, using passive techniques, are usually used as personal devices to attenuate noise in transportation, industry etc. However, these compact and light devices perform better for short wavelength noise than for long wavelength noise, i.e. low frequency noise. Active noise control (ANC) was introduced as a solution to attenuate low frequency noises, generally bellow 500 Hz. An ANC system combines a secondary noise (anti-noise) of opposite phase with the primary noise (unwanted noise), resulting in cancellation of both noises, as seen in Figure 1. However, ANC does not perform well for high frequency noises so, both passive and active techniques are used to complement each other in order to achieve better noise-cancelling results [8]. An ANC headset is an example of application where this is employed.

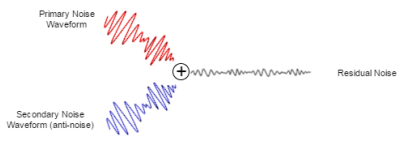

Figure 1: Active noise cancellation concept.

A generic ANC system, seen in Figure 2 is composed of an error microphone, to capture the noise resulting from the superposition, a loudspeaker as the anti-noise source, a reference microphone to give advanced information about the noise, in feedforward systems, and a controller to process the signals.

Most commercial headsets are based on an analogue filter controller [3]. Their use is advantageous for their stability, low system delay, low power consumption, small hardware size, simple control algorithm and good attenuation of random and impulse noises (broadband noise)[8]. However, they are only applicable to linear time-invariant systems and are hard to design for multiple input, multiple output systems [4]. For most ANC applications, the physical system may have time varying acoustic and environmental characteristics thus the use of an adaptive controller is desired, to model these variations.

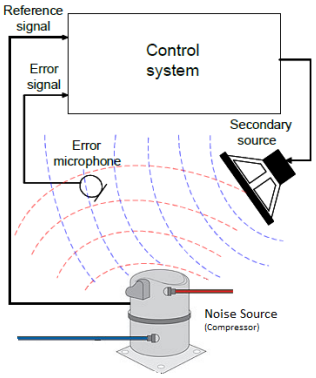

Figure 2: Basic blocks of a feedforward ANC system.

Adaptive controllers are generally implemented as adaptive filters in digital signal processors. These are digital filters whose coefficients are adjusted by an adaptive algorithm. Due to these system's self-optimizing and tracking capabilities, they have improved performance in a larger bandwidth over

fixed controllers with periodic and tonal noises (narrowband noise). Also, they are able to control multiple input and multiple output systems (multichannel systems). However, they are digital so the delays of the A/D and D/A converters are usually high, therefore their performance while cancelling broadband noise is inferior to fixed controllers.

The ideal result of ANC is no sound at all but, in reality, the actual noise cancellation depends on the accuracy of the data processing algorithm (calculations) to determine and synthesize the anti-noise and on the characteristics of the system. To improve those, new algorithms, hardware and system configurations should be developed and tested. A stable system is difficult to obtain for adaptive controllers, since there are multiple sources of instability for a ANC algorithm such as modelling errors, zeroes in inverse models, over driven systems, i.e. noises too low that exceeds the numerical range of a system.

One recent design is an ANC headset system employing both fixed controller and adaptive controller. The adaptive controller would reduce periodic signals while the fixed would control broadband signals [10, 7].

2. Background

In this section, the theoretical background necessary to understand the work is presented, namely the Least Mean Squares (LMS) algorithm, Filtered-X LMS (FxLMS) for a feedforward and feedback ANC system and its variations to solve the problem of secondary path modelling error.

2.1. Types of ANC systems

Active headsets can be interpreted as a problem of noise propagating in ducts, since plane waves in ducts and the sound field in a ear cup are both one-dimensional problems, thus enabling good results to be achieved with a single-channel control system [4]. For multi-dimensional noise fields it is necessary to employ a multiple-channel system.

There are two main configurations for ANC systems: feedback and feedforward. In addition, feedback types may be further classified into analogue (fixed) and digital (adaptive), depending on the controller used. Fixed controllers and multiple-channel systems are outside of the scope of this work.

Figure 3 illustrates a single channel feedforward system. It is composed by a controller, two microphones (reference and error) and a loudspeaker. It is the only configuration capable of cancelling broadband noise if the causality and high coherence conditions are met.

To ensure causality, the distance from the reference microphone to the error microphone should be greater than the distance from the secondary source to the error microphones. Also, the propagation time between the reference sensor and the secondary source should be larger than the time the controller takes to generate the anti-noise at the loudspeaker. To achieve high coherence between the reference signal and the primary noise, the reference microphone should be close to the noise source, in order to reduce the amount of ambient noise captured by the microphone. There can be acoustic feedback between the reference microphone and the secondary source in feedforward systems, but that should be low in headset systems.

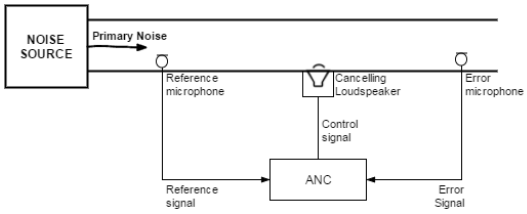

Figure 3: Single-channel feedforward ANC system in a duct.

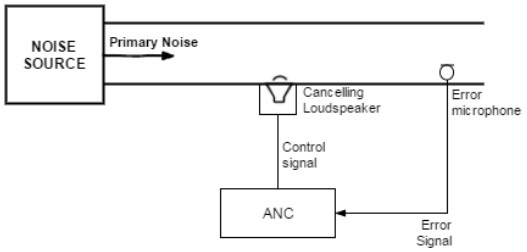

Figure 4: Single-channel feedback ANC system in a duct.

Adaptive feedback systems are composed of an error microphone and a secondary source. Since there is no reference microphone the reference signal has to be estimated by the system. Therefore, it can only cancel narrowband noise by exploiting their predictability. However, they only need one microphone and good references are hard to get and therefore are the most used conguration for headsets.. The only design constraint is the choice and positioning of the loudspeaker and error microphone to improve stability and noise reduction.

2.2. Adaptive Controller

ANC can be seen under the system identification framework as seen in Figure 5.

It works by modelling the primary path $P(z)$, from the reference microphone to the error microphone, with an adaptive filter $W(z)$, composed of a digital filter and an adaptive algorithm. The algorithm is given a reference signal $x(n)$, already exciting $P(z)$, to excite the adaptive model $W(z)$. The adaptive algorithm adjusts the filter coefficients in

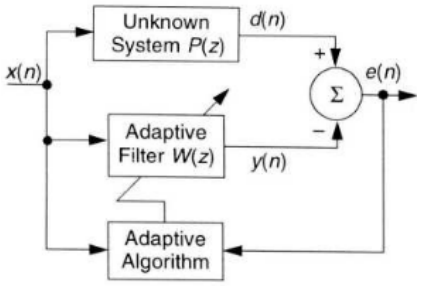

Figure 5: Adaptive system identification [8].

order to minimize the error signal $e(n)$, computed with the difference between the physical system response $d(n)$ and adaptive model response $y(n)$. When $e(n)$ has been minimized, the adaptive model ideally reproduces $P(z)$, implying that $y(n) = d(n)$.

The digital filter structure and the adaptive algorithm depend on the application requirements. The structure can be (transversal) finite impulse response (FIR), (recursive) infinite impulse response (IIR), lattice, among others. This work focuses on the Least Mean Squares (LMS) algorithm, however one of its variations, the Normalized LMS (NLMS), was used.

The LMS algorithm [2] updates a FIR filter coefficients with

$$\mathbf{w}(n+1) = \mathbf{w}(n) + \mu e(n)\mathbf{x}(n), \tag{1}$$

where μ is the step size, $\mathbf{w}(n)$ is the filter coefficients vector and $\mathbf{x}(n)$ is the filter input vector, both at time instant n. In order for this algorithm to be stable μ should verify

$$0 < \mu < \frac{2}{LP_x}, \tag{2}$$

where L is the adaptive filter length and P_x the power of the reference signal.

The stability condition of the LMS depends on $x(n)$. That inconvenience can be defeated by normalizing μ with respect to an estimate of the reference signal power, resulting in The NLMS algorithm 3.

$$\mathbf{w}(n+1) = \mathbf{w}(n) + \frac{\mu e(n)\mathbf{x}(n)}{\hat{P}_x(n)}. \tag{3}$$

where $\hat{}$ denotes estimate. $\hat{P}_x$ is computed with the squared euclidean norm, for NLMS algorithms as in the following expression

$$\hat{P}_x(n) = \|\mathbf{x}(n)\|^2 = \sum_{l=0}^{L-1} x^2(n-l). \tag{4}$$

This algorithm is faster than the ordinary LMS and it is convergent if the following condition on μ is satisfied.

$$0 < \mu < 2, \tag{5}$$

Another modified version of the LMS was used. It was the Leaky-LMS where a leakage factor λ tends to bias each coefficient toward zero. The principle of this method is similar to adding white noise to the input signal, prior to the adaptive filter [8]. It takes the form

$$\mathbf{w}(n+1) = \lambda\mathbf{w}(n) + \mu e(n)\mathbf{x}(n), \tag{6}$$

where λ is the leakage factor with $0 < \lambda \leq 1$. The value of the leakage factor is in general determined on an experimental basis, as a compromise between robustness and loss of performance of the adaptive filter, due to the white noise addition. Usually a good starting point is a leakage factor slightly less than 1.

2.3. ANC Algorithms

In a real ANC system, the error signal is not computed but is obtained by sampling the residual acoustic pressure resulting from the acoustic superposition of the noise and anti-noise. Therefore, in the path from the control signal $y(n)$ to the error signal $e(n)$, the devices have transfer functions which alter $y(n)$. This is called the secondary path $S(z)$ and the LMS algorithm should be modified to assure the system convergence.

The filtered-x LMS (FxLMS), illustrated in Figure 6, is one approach to compensate for the secondary path effects [8]. It filters the reference signal $x(n)$ with an estimate of the secondary path transfer function $\hat{S}(z)$ and inputs it in the NLMS along with the error signal. Therefore, an estimate of the secondary path transfer function must be available for the FxLMS algorithm.

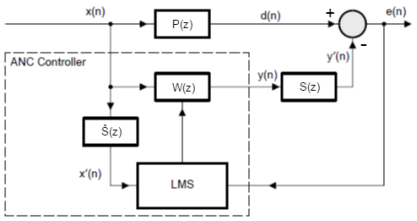

Figure 6: Block diagram of ANC system using the FxLMS algorithm [4].

The modelling of the secondary path transfer function is also a system identification problem. This time an internally generated white noise is used as a reference signal to construct the model $\hat{S}(z)$, during an initial stage. At the end of the training interval, the estimated model $S(z)$ is fixed and used for ANC operation. This is called the offline modelling technique, and it should be used if $S(z)$ is time-invariant. Even then, slight changes in the environment during system operation may happen which may lead the adaptive algorithm to instability if the phase difference between $S(z)$ and

$\hat{S}(z)$ has an excess of 90°. To solve this problem there, are two approaches one can take: to block noise control for frequencies whose phase error exceeds 90° more frequently; use the on-line modelling technique, usually employed in time varying secondary paths.

Adaptive on-line modelling of the secondary path should be used when $S(z)$ varies continuously in real time. $S(z)$ can be either occasionally or continuously estimated and the most recent estimate $\hat{S}(z)$ used in the weight update of the control filter $W(z)$. Provided that $S(z)$ changes slowly, the controller adaptation and secondary-path estimation functions can be considered separately. Two methods as generally used, the overall modelling algorithm (OMA) and the additive random noise algorithm.

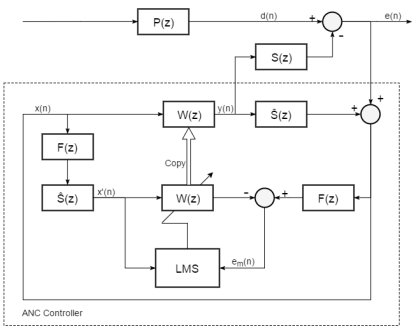

Figure 7: Block diagram of the feedback BMFxLMS algorithm.

Two FxLMS variations, which employ the approaches for the secondary path modelling error mentioned above, were used in this work. The feedback band-limited Modified FxLMS (BMFxLMS) [5], depicted in Figure 7, turns off the noise control by filtering out problematic frequencies of the primary noise $d(n)$, thus avoiding the instability associated to them. The frequencies where the modelling error is more frequent can be determined with a series of off-line modelling runs and computing the maximum phase difference between the estimates.

The MFxLMS is employed to obtain the electrical model of the noise cancelling because an acoustic signal cannot be electrically filtered. This is done by estimating the primary noise, adding an estimate of the anti-noise $\hat{y}'(n)$ to the error signal $e(n)$. Then, an estimate of the error signal, called modified error $e_m(n)$, is obtained with the difference between the primary noise estimate $\hat{d}(n)$ and the output of the filtered-x signal filtered by the current control filter. Now, it is possible to filter the reference signal $x(n)$ and $\hat{d}(n)$ by a bandpass filter $F(z)$, thus achieving the band limiting. This algorithm was implemented for a feedback configuration, by using $\hat{d}(n)$ as a reference signal, to later compare it with the feedback FxLMS.

The Mirrored MFxLMS [6], seen in Figure is a variation of the MFxLMS algorithm, with the OMA embedded in the algorithm for on-line modelling of the primary and secondary paths. It is stable even with incorrect secondary path models and deals very well with sudden changes. Instead of obtaining the electrical model of the noise cancellation as the regular MFxLMS, it passes the reference signal through the primary path estimate $\hat{P}(z)$ obtaining the primary noise estimate $\hat{d}(n)$.

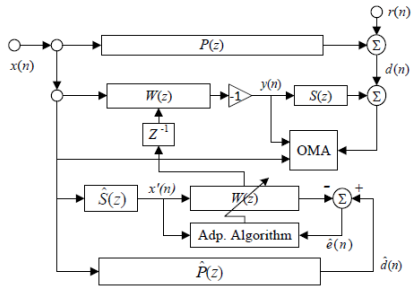

Figure 8: Block diagram of the MMFxLMS algorithm [6].

3. System architecture

3.1. Hardware

The developed system hardware is composed of a commercial ANC headset, the *ATH-ANC1 QuietPoint* ®, which had its control circuit removed, in order to use its microphones and loudspeakers. A development board, the TMS320C6713 DSP starter kit (C6713 DSK), Spectrum Digital, housing a TMS320C6713 floating-point digital signal processor (DSP) from Texas Instruments, was used as the substitute controller. The programs are downloaded to the DSK and the data is uploaded from the DSK with USB, through a JTAG emulator, to a Personal Computer.

The line-level channels were used as input and output of the board, meaning that no pre-amplifiers nor power amplifiers were available. So, a printed circuit board (PCB) containing the microphones' biasing, the microphones' pre-amplifiers, the power amplifiers to drive the loudspeakers and a power circuit to supply these circuits was produced. In order to implement the feedforward configuration, a reference microphone had to be assembled and the DSK_AUDIO4 daughtercard, from Educational DSP, LLC, was installed in the development board to expand the number of channels of the C6713 DSK. Then, the reference microphone biasing and pre-amplifier circuits were mounted on a breadboard. The analogue board developed is pictured in Figure 9.

The DSK_AUDIO4 daughtercard contains two 16 bit Coder Decoder (CODEC), each one with a

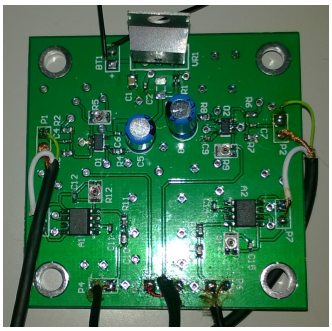

Figure 9: Analogue Circuit Developed.

stereo A/D converter (ADC) and a D/A converter (DAC). The maximum input and output of both devices is 1 V_{rms}. The error microphones have an estimated sensitivity of 13.2mV/Pa, and the pre-amplifiers have a gain of $A_{V_{\text{pre}}} = 55$, thus allowing to acquire noises with 2 Pa sound pressure, the maximum noise considered, without saturating the channel. The power amplifier has a gain of $Gv = 0.12$ outputting enough power for the loudspeakers to cancel a 2 Pa noise. The reference microphone pre-amplifier gain value was determined experimentally, to observe its impact on noise cancelling performance. The output of the error microphones pre-amplifiers were connected to the line-input of CODEC0 and input of the power amplifier connected to the line-output of the CODEC0. The output of the reference microphone pre-amplifier was connected to the line-input of CODEC1.

A diagram with the components of the system hardware is depicted in Figure 10.

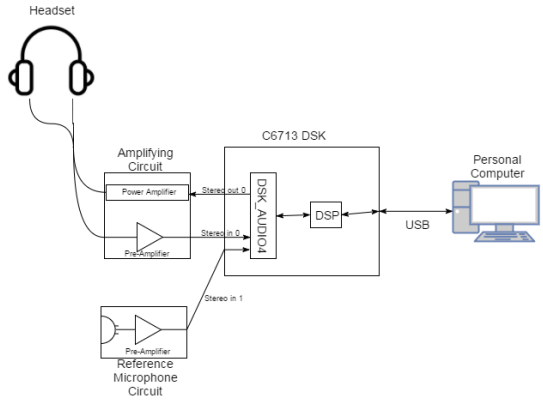

Figure 10: Diagram of ANC Headset System Hardware.

The error and reference signals were acquired at a sampling rate of $F_s = 16kHz$.

3.2. Software

The software was developed in Code Composer Studio software suite, version 6.1.0. All the programs were implemented in C-language.

Multi-rate signal processing was used to obtain the low delay of high sampling rates and the high processing time, i.e. the time spent by the processor doing the ANC algorithm computations, and lower adaptive filter order of low sampling rates. The 16 kHz sampling rate of the CODECs was decimated to the 2 kHz operating frequency of the ANC algorithms operated, meaning a conversion factor of 8 was used. The anti-aliasing/anti-image filters used were 161st order lowpass FIR filters with 500 Hz as cut-off frequency and 1000 Hz stopband corner frequency, with low ripple.

FxLMS algorithm was implemented for both feedforward and feedback system. For feedback FxLMS, the reference signal was synthesized by adding an estimate of the anti-noise $\hat{y}'(n) = y(n) * \hat{s}(n)$ to the error signal, obtaining a primary noise estimate which was used as the reference signal. It used NLMS with the power of the filtered-x as a normalizing factor.

Off-line secondary path estimation also used the NLMS, with the step-size $\mu_s = 0.01$ normalized by the power of the internally generated white noise, the training signal. This training signal was used to achieve fast convergence of the off-line modelling algorithm.

BMFxLMS algorithm uses the modified error signal, with the primary noise estimate band limited, and filtered-x signal also band limited as the NLMS input. The normalizing factor was the bandlimited filtered-x power. The phase error was found to be above 90° for frequencies under 80 Hz. The band limiting filter was implemented using a linear phase FIR filter. It had cut off frequencies of 100 and 500 Hz and stopband corner frequencies of 25 and 900 Hz and relatively high ripple comparing to the decimator and interpolator filters. The resulting filter was a 60th order bandpass filter.

The MMFxLMS algorithm [6] was implemented in C-language.

The step sizes, filter lengths and leakage factors of all algorithms were determined experimentally to achieve the best performance in an experiment explained in the following section.

4. Results

Various real-time tests were performed to understand the capabilities of the system. All the experiments had a user wearing the headset and the data was acquired by plotting the systems signals in the graphing tool of CCS, exporting that data and process it in MATLAB. The secondary paths of the system were characterized, with the secondary path modelling error being estimated. Then each algorithm went through a process of changing various system parameters, with the resulting performance assessed.

4.1. Secondary path characterization
The parameters, amplifier gains, step-sizes, sampling frequency, etc., used at the time of the measurements presented in this subsection were not the ones in the final system. Nevertheless they are useful to make some conclusions.

Audio system measurements

After the assembly of the system hardware, i.e. the stereo headset, DSK board and analogue amplifier circuit, some of the systems audio characteristics were measured to know to what extent the hardware affects the system performance.

The electrical crosstalk of the DSK was studied. It measured the introduction of electrical noise in one channel, when another channel is excited by a signal. More specifically, the DAC emitted a signal to drive the loudspeaker and the signal sampled by the ADC was observed. There was no considerable electrical crosstalk between the channels. However, these results had little significance because the analogue circuit was not included in the measurement.

To study the non-linear distortion, the off-line secondary path modelling had the training signal maximum amplitude increased with the values $\{5000, 10000, 15000, 20000\}$. Each run used a value and the resulting error signal power would be observed. If, with each variation of input power, the output power does not increase in the same way, there are non-linearities present in the circuit. It was observed a linear relationship between the input and output powers except for the lowest digital gain used, Gd = 5k, which exhibited high non linearity for low power signals.

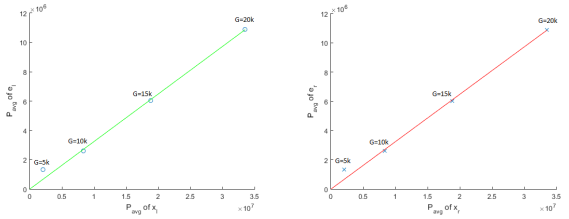

(a) Left Channel (b) Right Channel

Figure 11: Secondary path Input-Output linearity.

To determine the total harmonic distortion (THD), a sinusoidal signal, with frequencies $f \in \{50, 75, 100, 250, 500, 750, 1000\}Hz$ for each run, was input in the secondary path and the output THD, using the harmonics of the input signal frequency, was computed. A linear system with a sinusoidal signal as input has always a sinusoidal signal with the same frequency at the output. THD is a measurement of the extent of non-linear distortion. As seen in Figure 12, frequencies below or equal to 100 Hz had THD between 1% and 2%. The rest of

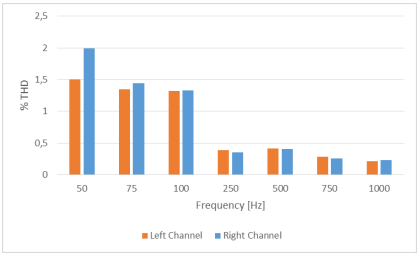

Figure 12: Total harmonic distortion of the secondary path.

the frequencies had THD below 1%. The THD results were found to be satisfactory because 1% distortion will be only noticeable for noise cancelling levels close to 40 dB, which is a great deal more than what is expected for the attenuation performance of this system.

4.2. Secondary path off-line modelling
To learn about the off-line secondary path modelling algorithm performance, 100 runs of the algorithm were realized. Then the phase error between the secondary path and the estimates was computed. It should be noted that the sampling frequency used for these measurements

Figure 13 shows the acquired impulse responses. Each line represents an estimate of the secondary path. It can be seen that there is great precision in modelling the delay of the secondary path, i.e. the large peak, because on that point the estimates are not spread. Thus, one can conclude that there is a big possibility of the algorithm accurately estimating the secondary path delay. However there is a big spread on the signal segment after the peak which may result in instability in the system.

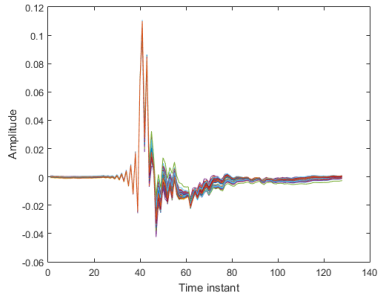

Figure 13: Estimated secondary path impulse responses.

Figure 14 shows that there is a big variation of phase on the lower end of the spectrum. More specifically, approximately under 80 Hz the phase error is above 90° thus, at these frequencies the system should be more prone to instability or at least slower convergence. This is was expected because

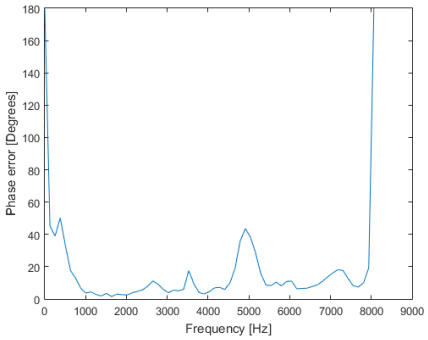

(a) Maximum difference between the secondary path estimates phase.

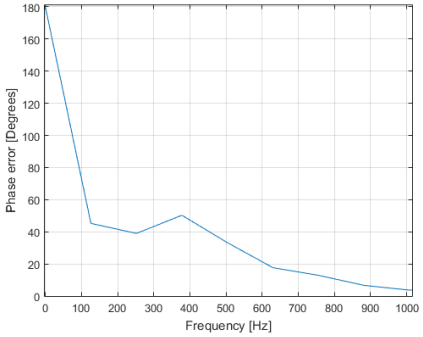

(b) Detail on the phase error plot of the secondary path estimates.

Figure 14: Phase error of the secondary path estimates.

at low frequencies the secondary path has small amplitude therefore the signal to noise ratio is low in these frequencies.

4.3. Algorithm performance evaluation

The experimental setup for the parameter optimization is depicted in Figure 15. This setup was used for all the algorithms and the presented distances were used in an effort to meet the causality condition and high coherency condition. Even though it depicts a feedforward system, the reference microphone was turned off when using feedback algorithms. The noise source utilized was a Pioneer XR-NM1 stereo system.

For each algorithm a good combination of parameter values, which gave good performance, was found. Then that set of parameters was used in various tests where the primary noise was changed.

Experimental parameter optimization

In this procedure the system parameters were manipulated to achieve the best possible performance. The parameters to be set were the step size μ, the leakage factor λ, the adaptive filters length $L_w = L_s$ and the reference microphone preamplifier gain $A_{V_{\text{ref}}}$. A sinusoidal noise with 100 Hz

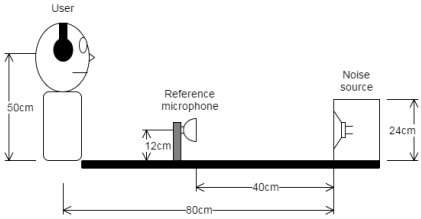

Figure 15: Experimental setup of the performance evaluation.

was used a the primary noise. Two levels of sound pressure were used to test the performance at high sound pressure levels and low sound pressure levels.

The sampling frequency was also varied not with optimization in mind but to see how the performance varied with it. The sampling frequencies tested were 16 kHz without decimation, 8 kHz decimated from 48 kHz and 2 kHz decimated from 16 kHz.

Data was gathered while varying one of these variables and holding all others at a constant value to best isolate its effect on the system. Performance was assessed by observing 4 different performance measures: attenuation, convergence time, stability and robustness. To measure stability a subjective method of classification was employed with grades being stable, oscillating, unstable, very unstable, diverging. A system configuration was classified with one grade based on the amount of runs it displayed a certain behaviour. Robustness was determined by inducing perturbations to the headset, specifically taking off and putting on the headset. Attenuation was the favoured measure to choose the best value, then it was convergence time, stability and for last robustness.

The resulting parameters of the optimization process are presented in Table 1. They were not necessarily the best combination of parameters since the study was incomplete, but presented a good balance of attenuation, stability and speed while cancelling both high level noises and low level noises.

This study proved valuable to understand the weight some parameters have on the performance measures used. The system revealed to be more unstable for high sound pressure levels, with this effect being mitigated by using the leakage factor. However, it limits the output power of the system, thus reducing attenuation in the process. The lowest pre-amplifier gain generated the highest attenuation. The convergence time increased with the filter length. The convergence time decreased as the step size increased. For the sampling frequency, stability and robustness was worse without multi-rate processing. With multi-rate processing, attenuation was higher for 8 kHz but the stability and robustness was better with 2 kHz for some algo-

rithms, namely the BMFxLMS algorithm.

Table 1: Parameters obtained from the experimental parameter optimization.

	μ	λ	$L_w = L_s$	$A_{V_{\text{ref}}}$
FxLMS_fb	0,005	1	120	-
BMFxLMS	0,005	1	55	-
FxLMS_ff	0,005	1	200	62,5
MMFxLMS	1	1	200	62,5

Tone frequency sweep

In this set of experiments the sinusoidal noise had its frequency varied. The resulting attenuation was noted and other relevant measures of performance observed. Table 2 has a comparison of the attenuation results for each algorithm.

On average, the best attenuation is from the BMFxLMS and the worse from the MMFxLMS. The feedback FxLMS algorithm was the least stable and the MMFxLMS was the most stable. From these results, it can be concluded that the methods to counter the modelling error effects were successful in doing so.

Comparing to the literature results [9, 1], even though the system can achieve good attenuation levels, superior to 30 dB, the results reported could get over 40 dB of attenuation. This can be explained by their methods employed to obtain the attenuation measures. Their attenuated noises were acquired inside head simulators with high precision microphones, whereas in this work the residual signal, contaminated by background noise, was used as the attenuated noise. The fixed controller headset tested in [1] revealed to be inferior, however it is a very old model.

Narrowband noise

In this procedure the primary noise used was an industrial compressor, with narrowband spectrum. Some high power harmonics were observed for the trials of each algorithm and their attenuation compared. In Table 3 the attenuation for the observed harmonics and the total attenuation are presented, for each algorithm.

The feedforward FxLMS had the best total attenuation and on average of the observed harmonics. The spectrum of this algorithm attenuation can be seen in Figure 16. MMFxLMS had equally good average attenuation for those harmonics, however the overall performance was not very good. Although the feedback FxLMS had the second best total attenuation, it was the algorithm with the worst stability. The BMFxLMS improved on it but had the worst attenuation of harmonics. The feedforward algorithms had no stability issues.

The results of the prototypes reported in other works [11, 9] show that, although the present system has a worse total attenuation, the attenuation for harmonics higher than 100 Hz is comparable and for harmonics higher than 200 Hz is superior. In those works commercial analogue headsets had their attenuation assessed. The system developed in this work had performance similar to that of the commercial headsets, therefore the results were good.

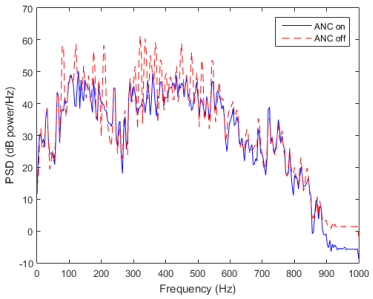

Figure 16: Power spectra of narrowband noise with and without ANC, for feedforward FxLMS.

Broadband Noise

Broadband noise was not cancelled by this system. Figure 17 depicts the situation for the algorithm which had the best performance, the feedforward FxLMS, since it did not increase the noise level in the system. For feedback systems that was expected, due to their inability to cancel those noise. The physical placement of the sensors for the feedforward systems probably did not meet the coherence and causality conditions.

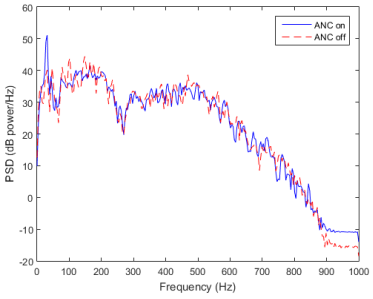

Figure 17: Power spectra of broadband noise with and without ANC, for feedforward FxLMS.

5. Conclusions

The active headset system, with both feedback and feedforward configurations, showed satisfactory attenuation. Not only it reinforced the fact that feedforward systems perform better than feedback systems, but also demonstrated the superior attenuation of an adaptive controller compared to some

Table 2: Attenuation of the algorithms with the tone frequency sweep. fb - algorithm for feedback system; ff - algorithm for feedforward system.

Frequency [Hz]	FxLMS_fb[dB]	BMFxLMS[dB]	FxLMS_ff[dB]	MMFxLMS[dB]
60	21,62	23,73	19,62	16,62
100	28,83	18,94	26,69	29,6
200	28,27	28,45	20,52	29,72
400	26,58	24,9	28,23	23,77
500	26,35	38,93	32,37	25,03

Table 3: Attenuation of the algorithms with the narrowband noise. fb - algorithm for feedback system; ff - algorithm for feedforward system.

Frequency [Hz]	FxLMS_fb-Att[dB]	BMFxLMS-Att[dB]	FxLMS_ff-Att[dB]	MMFxLMS-Att[dB]
82	11,06	3,65	20.45	23.41
121	10,88	9,35	19.62	20.02
175,8	9,38	6,18	8.74	8
207	18,35	8,12	18.63	15.13
320	18,35	-	22.29	21.13
Total Attenuation	5.42	1.13	7.1	1.07

fixed controllers, seen in the consulted literature. However, it revealed instability issues related to the modelling error of the secondary path estimates, inherent to the off-line modelling method.

The two approaches used to reduce the effects of the phase error were successful mitigating them. The instability of the FxLMS algorithm was reduced, however at the cost of reduced attenuation for real noises. Still, the BMFxLMS was not completely stable and it presented great lack of robustness. The MMFxLMS revealed to be robust to all perturbations but the take off/put on situation, it was very stable when the numerical range of the CODEC was not exceeded by the overshoot inherent to it. This overshoot was the greatest drawback of this algorithm, since, as stated, it also degraded its attenuation for real systems.

It should be noted that the tone frequency sweep, narrowband and broadband noises all used loud noises, to maximize the attenuation achieved. However, at these sound pressure levels, the stability of the system got worse.

The experimental results are acceptable since it compares to, and sometimes it exceeds, the performance of the reported commercial analogue systems, however it obtained inferior attenuation compared to recent results from other researchers. The system presents stability issues, which can difficult a commercial application, thus they should be better studied.

It was made evident how important is a closer study of causality and coherence to achieve broadband cancellation. For instance it would be useful to measure the electrical delay of the CODEC and compare to the acoustic delay of the system, to better study the causality of the system. Also a study of the position of the reference microphone and its effect on the performance of broadband noise cancellation would be in order.

References

[1] W. R. A.K. Wang, B. Tse. Adaptive active noise control for headphones using the tms320c30 dsp. Technical report, Texas instruments, January 1997. spra160.

[2] S. S. B. Widrow. *Adaptive Signal Processing*. Prentice-Hall, 1^{st} edition, 1985.

[3] C. Hansen. *Understanding Active Noise Cancellation*. CRC Press, 1^{st} edition, 2001.

[4] C. Hansen. *Active Control of Noise and Vibration*. CRC Press, 1^{st} edition, 2012.

[5] P. Lopes. Active noise control algorithms with reduced channel count and their stability analysis. *Signal Processing*, 88(4):811–821, Apr. 2008.

[6] M. P. P.A.C. Lopes, J. Gerald. The mmfxlms algorithm for active noise control with on-line secondary path modelling. *Digital Signal Processing*, 60:75–80, Jan. 2017.

[7] T. Schumacher, H. Krger, M. Jeub, P. Vary, and C. Beaugeant. Active noise control in headsets: A new approach for broadband feedback anc. In *2011 IEEE International Conference on Acoustics, Speech and Signal Processing (ICASSP)*, pages 417–420, May 2011.

[8] D. M. S.M. Kuo. *Active Noise Control Systems: Algorithms and DSP Implementations*. New York: Wiley, 1^{st} edition, 1996.

[9] W. G. S.M.Kuo, S. Mitra. Active noise control system for headphone applications. *IEEE Transactions on Control Systems Technology*, 14(2):331–335, March 2006.

[10] Y. Song, Y. Gong, and S. M. Kuo. A robust hybrid feedback active noise cancellation headset. *IEEE Transactions on Speech and Audio Processing*, 13(4):607–617, July 2005.

[11] A. Tokatli. Design and implementation of a dsp based active noise controler for headsets. Master's thesis, The Middle East Technical University, August 2004.